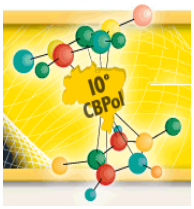

STUDY OF THE MORPHOLOGY EXHIBITED BY LINEAR SEGMENTED POLYURETHANES

I. M. Pereira[1,2]; R. L. Oréfice[2*]

[1]*Centro Federal de Educação Tecnológica de Minas Gerais – CEFET/MG – Timóteo-MG*

[2]*Departamento de Engenharia Metalúrgica e de Materiais – Universidade Federal de Minas Gerais – UFMG, Belo Horizonte-MG* – rorefice@demet.ufmg.br

Five series of segmented polyurethanes with different hard segment content were prepared by the prepolymer mixing method. The nano-morphology of the obtained polyurethanes and their microphase separation were investigated by infrared spectroscopy, modulated differential scanning calorimetry and small-angle X-ray scattering. Although highly hydrogen bonded hard segments were formed, high hard segment contents promoted phase mixture and decreased the chain mobility, decreasing the hard segment domain precipitation and the soft segments crystallization. The applied techniques were able to show that the hard-segment content and the hard-segment interactions were the two controlling factors for determining the structure of segmented polyurethanes.

Keywords: *Segmented polyurethanes, SAXS, microphase separation, and nano-morphology*

Introduction

Segmented polyurethanes (PUs) are multiblock copolymers which consist of the so-called hard (polar) and soft (nonpolar) segments. The multi-phase structure of PUs results from the repulsive interaction between dissimilar segments and thermodynamic immiscibility of hard and soft segments at low temperature. The microphase separation structure of PUs depends on many factors, i.e.: structure and molecular weight of the soft segment, nature of chain extender, hard segment content and interactions, thermal and solvent history during sample preparation[1-4]. In the present work, PUs were synthesized in an aqueous environment by combining hard segments derived from aliphatic isophorone diisocyanate with soft segments based on poly(caprolactone diol). Five series of PUs having different hard segment contents were synthesized. The infrared spectroscopy (IRS), modulated differential scanning calorimetry (MDSC) and the small-angle X-ray scattering (SAXS) were used to provide information of the nano-morphology of the obtained PUs and on their microphase separation.

Materials and Methods

Prepolymer synthesis

Poly(caprolactone diol) (PCL – Mn = 530, 1250, 2000, 10000 g mol^{-1}), isophorone diisocyanate (IPDI), 2,2-bis(hydroxymethyl), propionic acid (DMPA) and dibutyl tin dilaurate (DBDLT) were

obtained from Aldrich (St. Louis, MO). Triethylamine (TEA, 98%) and hydrazine (HZ, 25%) were purchased from Vetec (RJ, Brazil). All these chemicals were employed throughout this work without any previous treatment. PUs were prepared by the prepolymer mixing method, according to a procedure described in previous work[5]. The feed ratios are shown in Table 1, where $W(HS)$ is weight fraction of soft segment content, obtained according to Eq. 1.

$$W(HS) = \frac{Weight_{IPDI} + Weight_{HZ}}{Weight_{PU}} \times 100 \quad (1)$$

Table 1 – Composition (wt.%) of waterborne PUs

	PCL				DMPA	IPDI	HZ	TEA	$W(HS)$
	530	1250	2000	10000					
PU530	34.3	–	–	–	6.6	50.5	3.6	4.9	57.0
PU1250	–	55.4	–	–	4.5	34.6	2.1	3.4	38.0
PU2000	–	–	66.1	–	3.3	25.8	1.9	3.0	28.5
PU10000&530	7.1	–	–	72.0	2.1	16.1	1.2	1.6	17.5
PU10000	–	–	–	90.8	0.9	7.1	0.5	0.7	7.6

Infrared spectroscopy

Infrared spectra were collected in a Fourier transform infrared spectrophotometer (FTIR; Perkin–Elmer, model Spectrum 1000). Measurements were carried out using the attenuated total reflectance (ATR) technique. Each spectrum was a result of 64 scans with a resolution of 4 cm^{-1}.

Modulated differential scanning calorimetry (MDSC)

MDSC measurements were performed using a TA Instruments 2920. The following protocol was applied to each sample: (1) heating from room temperature to 110°C at 15°C min^{-1}, (2) holding for 3.00min at 110°C, (3) cooling to -110°C at 3.00°C/min, modulating +/- 1.00°C every 60 seconds. The glass transition temperature (T_g) were obtained by the analyzing software of the calorimeter.

Synchrotron small angle X-ray scattering (SAXS)

SAXS measurements of synchrotron small angle X-ray scattering were performed using the beam line of the National Synchrotron Light Laboratory (LNLS, Campinas, Brazil). After passing through a thin beryllium window, the beam is monochromatized ($\lambda = 1.488$ Å) and horizontally focused by a cylindrically bent and asymmetrically cut silicon single crystal. The X-ray scattering intensity, $I_{(q)}$, was experimentally determined as a function of the scattering vector, q, whose modulus is given by Eq. 2:

$$q = \frac{4\pi}{\lambda}\sin\theta \qquad (2)$$

where λ is the X-ray wavelength and θ is half the scattering angle.

Each SAXS pattern corresponds to a data collection time of 900 s. From the experimental scattering intensity produced by all the studied samples, the parasitic scattering intensity produced by the collimating slits was subtracted. All SAXS patterns were corrected for the non-constant sensitivity of the PSD, for the time varying intensity of the direct synchrotron beam and for differences in sample thickness. Because of the normalization procedure, the SAXS intensity was determined for all samples in the same arbitrary units so that they can be directly compared. The sample-detector distance of 551.6 mm was used during the measurements.

Results and discussion

Typical infrared spectra of obtained PUs are shown in Figure 1. It was observed that the position of the absorption bands of each specific functional group was similar for all obtained PUs.

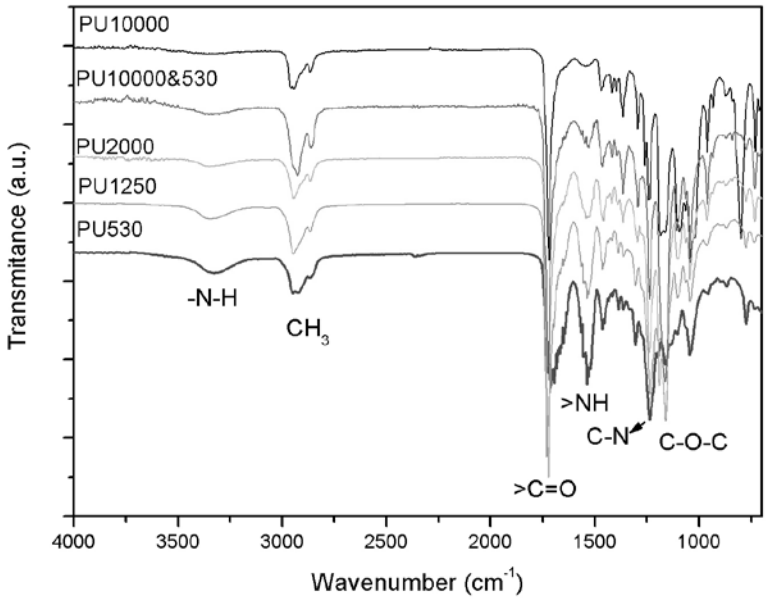

Figure 1 – FTIR spectra of PU530, PU1250, PU2000, PU10000&530 and PU10000 samples

The primary amine stretching modes appear at 3600–3150cm^{-1}. The absorption band at about ~3300cm^{-1} corresponds to hydrogen bonded –N–H group and absorption at ~3500cm^{-1} to nonbonded –N–H. The carbonyl group stretching vibrations, C=O, appear at 1760–1600cm^{-1}. A series of specific absorption bands are present within the 1760–1600cm^{-1} broad band, such as the absorption band due to the ester bond from PCL soft segments and others associated with multiple interactions between urea and urethane bonds and –N–H groups. IR bands at ~1720cm^{-1}, ~1700cm^{-}

[1], ~1660cm^{-1}, ~1630cm^{-1} are assigned, respectively, to free urethane stretching band, hydrogen bonded urethane stretching band, free urea stretching band and hydrogen bonded urea stretching band. The secondary amide absorption, >N–H, appears at 1640–1540cm^{-1}. The band at 1150cm^{-1} is assigned to the stretching of the –C–O–C– group[5].

Hydrogen bonding is known as an important driving force for the phase separation of a hard segment from a soft-segment matrix. Thus, the carbonyl region usually has been investigated for the quantitative study of microphase separation or mixing in PU[6]. However, two main spectral regions are of interest in studying the hydrogen bonding of segmented PUs: N–H and C=O, respectively, absorption primary amine stretching and carbonyl group stretching. Since band overlapping is observed, a deconvolution mathematical procedure (by using the PickFiT® software) was performed on spectra of Figure 1 to enhance resolution of each individual band. The separated curves are shown in Figure 2. Results are summarized in Table 2.

The extent of the –NH groups participating in hydrogen bonding could be expressed by a (–NH) hydrogen-bonding index $HBI^{(\%)}_{(-NH)}$, Eq. 3.

$$HBI^{(\%)}_{(-NH)} = \frac{NH_{Bonded}}{NH_{Bonded} + NH_{Free}} \times 100 \qquad (3)$$

where NH_{Bonded} and NH_{Free} are respectively the band peak area of free and bonded –NH groups.

The extent of the carbonyl absorption groups participating in hydrogen bonding could be expressed by a hydrogen-bonding index $HBI^{(\%)}_{(C=O)}$, which is the fraction of hydrogen bonded in the carbonyl groups stretching vibrations Eq. 4[7-9].

$$HBI^{(\%)}_{(C=O)} = \frac{A_{1700} + A_{1640}}{A_{1700} + A_{1640} + A_{1724} + A_{1660}} \times 100 \qquad (4)$$

where A_{1724}, A_{1700}, A_{1660}, and A_{1640} are respectively the band peak area of free urethane, bonded urethane, free urea, bonded urea and ester.

The degree of phase mixture, $DPM(\%)$, can be calculated from fraction of hard segment dissolved in soft domain, and their ratio is designated by Eq 5[7]. Results are summarized in Table 2.

$$DPM(\%) = \frac{\left(1 - HBI_{(C=O)}^{(\%)}\right) \times W(HS)}{\left(1 - HBI_{(C=O)}^{(\%)}\right) \times W(HS) + \left(1 - W(HS)\right)} \quad (5)$$

The bands 1160cm^{-1} and 1190cm^{-1} at Figure 1 are associated, respectively, with C–O amorphous and crystalline bands[10]. As band overlapping also occurs, deconvolution procedures were performed. The separated curves are shown in Figure 2. The FTIR crystallinity index, α_{FTIR}, was defined according to Eq. 6:

$$\alpha_{FTIR} = \frac{A_{1190}}{A_{1190} + A_{1160}} \times 100 \quad (6)$$

where A_{1190} and A_{1160} are respectively the band peak area of C–O amorphous and crystalline band.

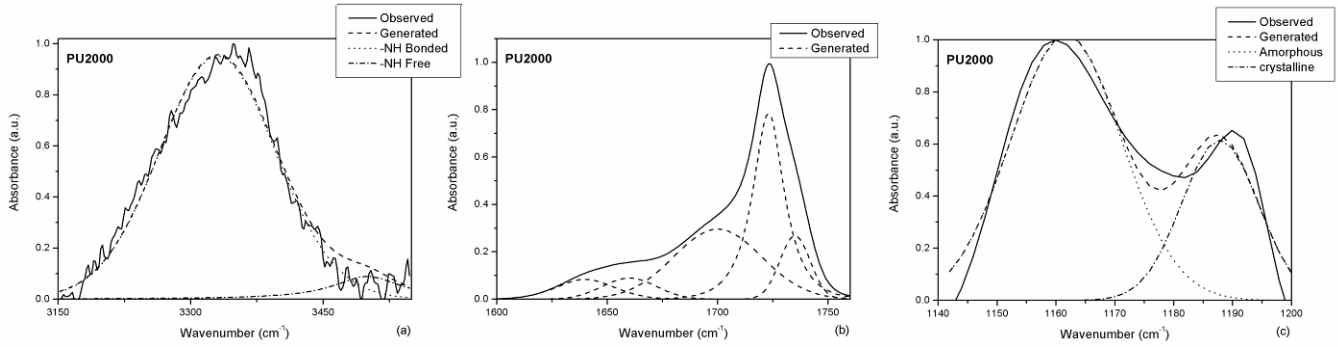

Figure 2 – Illustration of the deconvolution procedure used to determine the overlapped band of FTIR spectrum: (a) primary amine stretching, (b) carbonyl group stretching and (c) ether stretching.

Table 2 – FTIR results of as-molded poly(ester–urethanes)

	$HBI_{(-NH)}^{(\%)}$	$HBI_{(C=O)}^{(\%)}$	α_{FTIR}	DPM (%)
PU530	96.21	54.24	0.000	37.73
PU1250	98.95	46.27	6.77	24.76
PU2000	94.40	54.74	29.14	15.25
PU10000&530	85.38	46.55	41.57	10.17
PU10000	63.65	31.78	54.78	5.35

The multi-phase structure of PUs is a result of the repulsive interaction between dissimilar segments and thermodynamic immiscibility of hard and soft segments at low temperature[2, 3, 11].

A linear relationship between hard segment content and $DPM(\%)$ was observed, Figure 3(a). PUs having high hard segment, i.e. PU530, contents were produced by using low molar mass PCL oligomers that display higher levels of chain mobility. This enhanced mobility can be useful in allowing urethane and urea groups to align themselves to form hydrogen bonds. The highly

hydrogen bonded hard segments act as physical cross-links, restricting segmental motion of the polymer chain. However, it does not result in a more significant phase separation between hard and soft segments because the weight fraction of hard segment. On the other hand, the lower values of $HBI(\%)$ of PU10000 do not result in a more extensive phase mixing since the reduction in hydrogen bonding within hard segments was compensated by an increase in the amount of soft segments. The hard segment content controls also the total of NH groups hydrogen bonded, Figure 3(a).

Thermal properties are summarized in Table 3. The second order transition, T_g, is observed around –60°C. In DSC analysis, the width of transition zone provides a qualitative measure of phase homogeneity, and the variation in the magnitude of T_g can indicate the degree of microphase separation[12]. Higher degree of hard segment dissolved in the soft segment delays the phase transition moving T_g to higher values, Figure 3(b).

Table 3 – DSC results of obtained poly(ester urethane).

	T_g (°C)	T_{onset} (°C)	T_{end} (°C)	Zone width
PU1250	–46.09	–53.80	–33.58	20.22
PU2000	–54.51	–59.65	–46.45	13.20
PU10000&530	–57.66	–64.65	–45.53	19.12
PU10000	–60.22	–64.09	–53.09	11.00

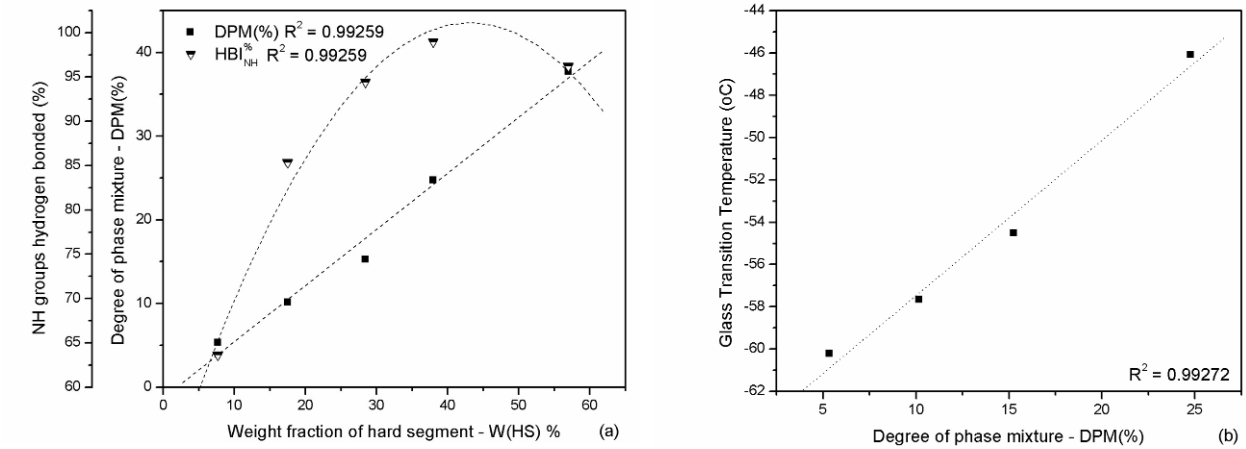

Figure 3 – (a) Influence of hard segment content on degree of phase mixture and (b) influence of the hard segment on glass transition

Figure 4 illustrates SAXS pattern of the obtained PUs. The patterns and intensity distribution of SAXS are dependent on the shape, the size and size distribution of scattering objects[13]. It is observed different nano-morphologies, varying from one phase system to multiphase polymer. The electron density of phase, reported by the scattering intensity, fluctuates from a low phase density to highly packed structures.

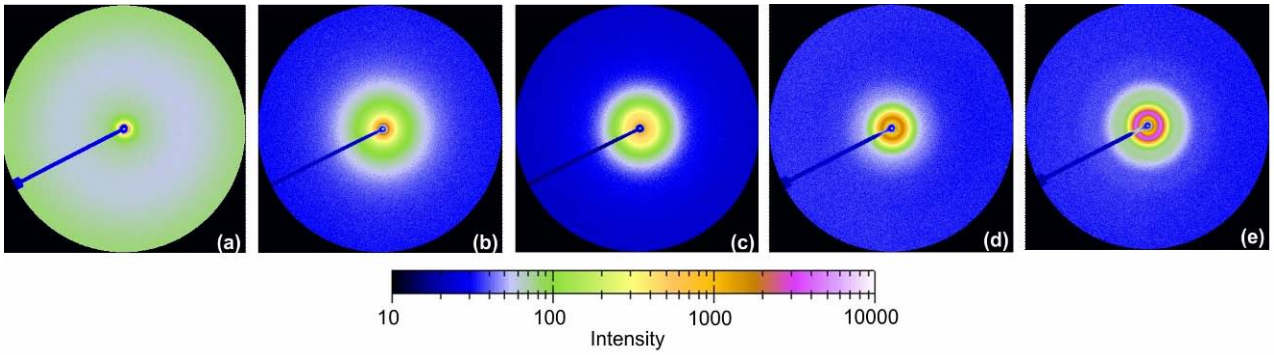

Figure 4 – SAXS pattern of: (a)PU530, (b)PU1250, (c)PU2000, (d)PU10000&530 and (e)PU10000.

Figure 5(a) illustrates SAXS data of the obtained PUs. The scattering peak observed in SAXS data of PU2000, PU10000&530 and PU10000 arises due to local heterogeneities in the electron density of the materials and it is usually interpreted as a consequence of the presence of distinct microphases with different electronic densities. However, to discuss the phase separation, it is convenient to employ the Lorentz correction, Q_{inv}, which describes the electron density fluctuation of polymer and is a good approximation to estimate the overall degree of phase separation in segmented polymers, Figure 5(b)[13-15]. The Lorentz correction, the invariant quantity, Q_{inv}, can be obtained by integrating $I_{(q)}q^2$ over the range of scattering angles, Eq. 7[13-15].

$$Q_{inv} = \int_0^\infty I_{(q)} q^2 dq \qquad (7)$$

where $I_{(q)}$ is X-ray scattering intensity and q the scattering vector.

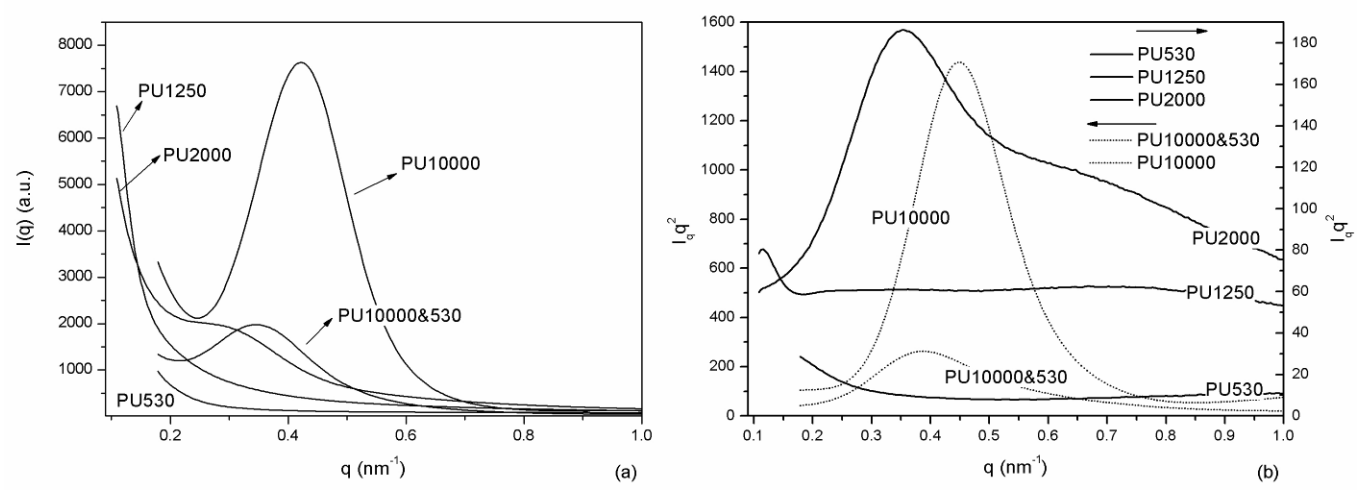

Figure 5 – (a) SAXS curves of obtained PUs and (b) Deconvoluted Lorentz SAXS pattern of samples

PU530 profile decreases monotonously with q, implying a high degree of phase mixture. The system can be thought as one phase structure. PU1250, PU2000, PU10000&530 and PU10000

present a multiphase structure including: amorphous matrix, hard domains and crystals. The contribution of each phase to the Lorentz corrected SAXS patterns were separated by a deconvolution procedure, Figure 6.

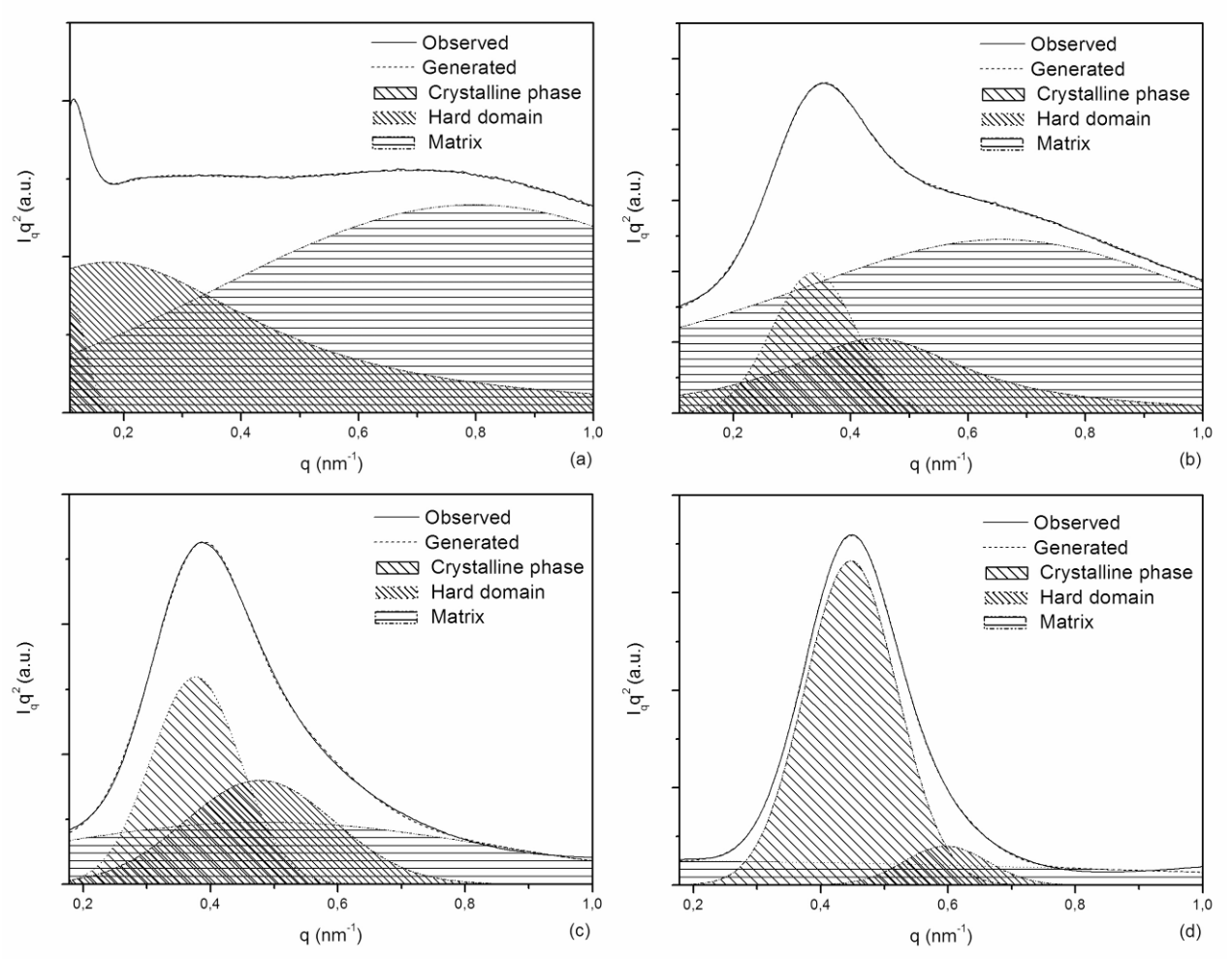

Figure 6 – Deconvoluted Lorentz SAXS patterns: (a)PU1250, (b)PU2000, (c)PU10000&530 and (d)PU10000.

Q_{inv} of each phase was obtained as fraction of the total area. The morphology of the polymer was investigated through the inter-domain repeat distance, L_{domain}, and/or lamellar crystalline repeat distance, $L_{Crystal}$. L is estimated from the $q_{\max}$ corresponding to the maximum of $I_{(q)}q^2$ versus q curves using Bragg's equation, Eq. 8[13-15]. Table 4 summarizes the results.

$$L = \frac{2\pi}{q_{\max}} \qquad (4)$$

Since Q_{inv} is obtained by integrating $I_{(q)}q^2$ over the range of scattering angles, phases with higher electron densities like crystals achieve higher integrated values. As indicated by α_{FTIR} and SAXS's

crystalline phase, PU10000&530 is more crystalline than PU2000, hence one should expected higher integrated values for PU10000&530 than PU2000. However, this is not observed, possibly because the presence of PCL530 in soft segments of PU10000&530 would restrict chain packing efficiency, resulting in the formation of a less perfectly crystal structure.

Table 4 – Deconvoluted SAXS results of crystalline phase, hard domains and matrix.

	Q_{inv}	Q_{inv} (%)			L (nm)	
		Crystalline phase	Hard Domain	Matrix	$L_{Crystal}$	L_{domain}
PU530	8.72	–	–	100.00	–	–
PU1250	54.48	1.72	31.48	66.80	55.30	35.97
PU2000	104.95	13.53	17.50	68.96	18.57	14.17
PU10000&530	82.83	33.70	28.25	38.05	16.69	13.17
PU10000	334.85	72.37	7.93	19.70	14.04	10.53

SAXS and FTIR results show good correlation. Q_{inv} describes the overall degree of phase separation or $100 - DPM(\%)$ (Figure 7-a) SAXS's crystalline phase measures α_{FTIR}, (Figure 7-b), and hard domain plus amorphous matrix represents $100 - \alpha_{FTIR}$, (Figure 7-c).

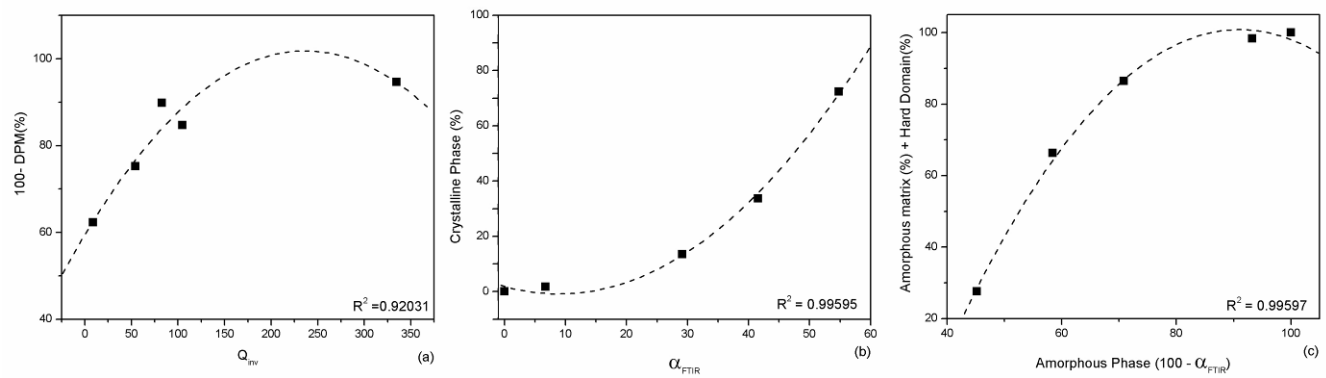

Figure 7 - Correlation between SAXS and FTIR results.

The $W(HS)$ influence on the microphase separation structure of PUs is illustrated in Figure 8(a). High segment contents promote phase mixture and decrease the chain mobility. Thus the soft segments are not able to align themselves to form crystals. The present results suggest that hard domain precipitation is controlled by H-bonding interactions, Figure 8(b).

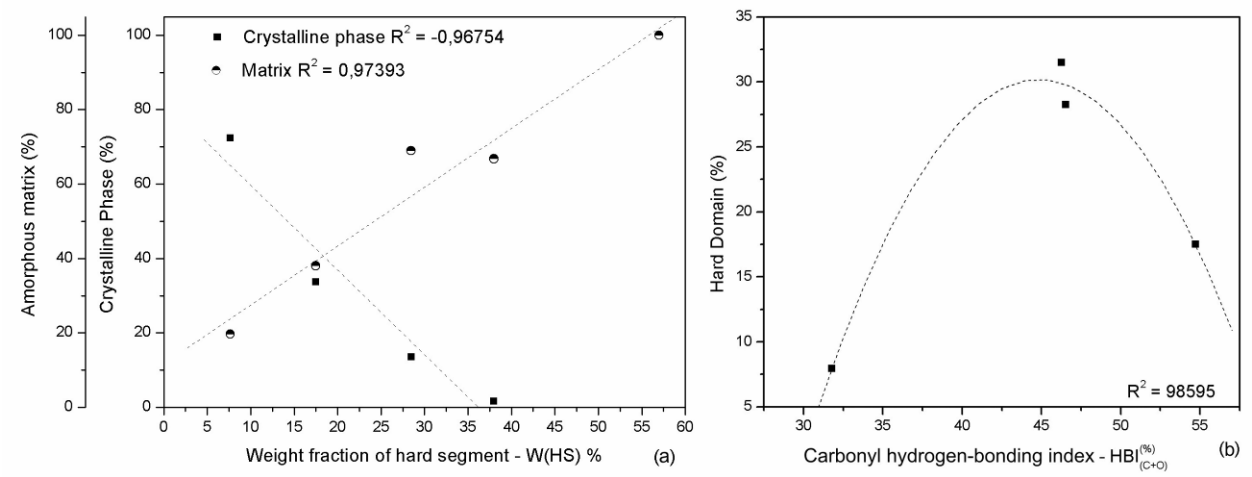

Figure 8 – Influence of hard segment content and $HBI^{(\%)}_{(C=O)}$ on the multiphase structure of polyurethane.

Conclusions

Polyurethane with multiphase structure including: amorphous matrix, hard domains and crystals were produced by altering the hard segment content. High segment contents promote phase mixture and decrease the chain mobility. Thus the soft segments are not able to align themselves to form crystals. SAXS results may be used to estimate the nano-morphology of segmented PUs.

Acknowledgments

The authors acknowledge the financial support from the following institutions: National Council for Scientific and Technological Development (CNPq), a foundation linked to the Ministry of Science and Technology (MCT) of the Brazilian Government; the State of Minas Gerais Research Foundation (FAPEMIG); and the National Synchrotron Light Laboratory (LNLS-Brazil) for the use of the SAXS beamline facilities.

References

1 – Nakamae K, Nishino T, Asaoka S, et al. Int J Adhes Adhes 1999;19(5):345–51.
2 – Pompe G, Pohlers A, Pötschke P, Pionteck J. Polymer 1998;39(21):5147–53.
3 – Lin JR, Chen LW. J Appl Polym Sci 1998;69(8):1563–74.
4 – Li YJ, Gao T, Liu J, et al. Macromolecules 1992;25(26):7365–72.
5 – Pereira IM, Patrício PSO, Oréfice RL in: 9º Congresso Brasileiro de Polímeros, Campina Grande, 2007, Vol. 1, 46.
6 – Cheong IW, Kong HC, An JH, Kim JH. J Polym Sci A 2004;42:4353–69.
7 – Liu Y, Pan C. Eur Polym J 1998;34(5-6):621–4.
8 – Cho JW, Lee SH. Eur Polym J 2004;40(7):1343–8.
9 – Ayres E, Oréfice RL, Yoshida, MI. Eur Polym J 2007;43(8):3510–21.
10 – Dillon J. Infrared Spectroscopy Atlas of Polyurethanes. Technomic Lancaster, PA, USA, 1989.
11 – Nakamae K, Nishino T, Asaoka S, et al. Int J Adhes Adhes 1999;19(5):345–51.
12 – Bao H, Zhang Z, Ying S. Polymer 1996;37(13):2751–4.
13 – Chang SL, Yu TL, Huang CC, et al. Polymer 1998;39(15):3479–89.
14 – Wang SH, Zhang Y, Ren WT, et al. Polymer Testing 2005;24(6):766–74.
15 – Li YJ, Kang WX, Stoffer JO, et al. Macromolecules 1994;27(2):612–4.